Journal of Assisted Reproduction and Genetics (2019) 36:1877–1890
https://doi.org/10.1007/s10815-019-01530-w

GAMETE BIOLOGY

Amyloid-like substance in mice and human oocytes and embryos

Ricardo N. Pimentel[1,2] · Paula A. Navarro[2] · Fang Wang[3] · LeRoy G. Robinson Jr.[3] · Michael Cammer[4] · Fengxia Liang[4] · Yael Kramer[3] · David Lawrence. Keefe[3]

Received: 6 May 2019 / Accepted: 9 July 2019 / Published online: 22 July 2019

Abstract

Purpose To identify and characterize amyloid-like substance (ALS) in human and mouse oocytes and preimplantation embryos.

Methods An experimental prospective pilot study. A total of 252 mouse oocytes and preimplantation embryos and 50 immature and in vitro matured human oocytes and parthenogenetic human embryos, from 11 consenting fertility patients, ages 18–45. Fluorescence intensity from immunofluorescent staining and data from confocal microscopy were quantified. Data were compared by one-way analysis of variance, with the least square-MEANS post-test, Pearson correlation coefficients (r), and bivariate analyses (t tests). ALS morphology was verified using transmission electron microscopy.

Results Immunostaining for ALS appears throughout the zona pellucida, as well as in the cytoplasm and nucleus of mouse and human oocytes, polar bodies, and parthenogenetic embryos, and mouse preimplantation embryos. In mouse, 2-cell embryos exhibited the highest level of ALS (69000187.4 ± 6733098.07). Electron microscopy confirmed the presence of ALS. In humans, fresh germinal vesicle stage oocytes exhibited the highest level of ALS (4164.74088 ± 1573.46) followed by metaphase I and II stages ($p = 0.008$). There was a significant negative association between levels of ALS and patient body mass index, number of days of ovarian stimulation, dose of gonadotropin used, time between retrieval and fixation, and time after the hCG trigger. Significantly higher levels of ALS were found in patients with AMH between 1 and 3 ng/ml compared to < 1 ng/ml.

Conclusion We demonstrate for the first time the presence, distribution, and change in ALS throughout some stages of mouse and human oocyte maturation and embryonic development. We also determine associations between ALS in human oocytes with clinical characteristics.

Keywords Amyloid · Oocyte quality · Reproductive aging · female fertility

Introduction

Mammalian oocytes are unique among germ cells in that they are exceptionally long-lived, and they age precociously. Unlike men, who continue to produce sperm throughout their lives, females halt oogenesis by about 20 weeks of gestation [1]. Primordial follicles, containing oocytes arrested at the diplotene stage of the first meiotic division, remain in a state of partial metabolic quiescence throughout the reproductive lifespan of the woman [2]. By birth, 75% of the follicular pool already has been lost and does not regenerate [3]. Follicular depletion accelerates at puberty and continues until near complete depletion at menopause. During the reproductive phase, about 1000 follicles activate each month, though only one becomes dominant and ovulates. The remainder undergoes atresia [4].

In addition to declining ovarian reserve, women experience decreasing fertility with age, which accelerates after age 35

Electronic supplementary material The online version of this article (https://doi.org/10.1007/s10815-019-01530-w) contains supplementary material, which is available to authorized users.

✉ David Lawrence. Keefe
david.keefe@nyumc.org

[1] Research Scientist from the Department of Obstetrics and Gynecology, New York University School of Medicine, 550 First Avenue, NBV 9N1, New York, NY, USA

[2] Present address: Human Reproduction Division, Department of Obstetrics and Gynecology, Faculty of Medicine of Ribeirao Preto, University of Sao Paulo, Ribeirao Preto, SP, Brazil

[3] Department of Obstetrics and Gynecology, Langone Medical Center, New York University, New York, NY, USA

[4] DART Microscopy Laboratory, New York University School of Medicine, New York, NY, USA

[5]. The oocyte must be the locus of reproductive aging, since donation of oocytes from young to older women abrogates the effects of aging on their fertility. The outcome of ART (Assisted Reproductive Technology), when using a women's own eggs, exhibits profound effects of aging [6]. This sharp decline in fertility with age results from decreasing oocyte developmental competence, which is the main determinant of embryo developmental competence and implantation rates [7, 8]. Markers of oocyte developmental competence are needed to help women make important clinical decisions [9–13]. Cellular and molecular mechanisms driving oocyte aging remain poorly understood. For this reason, maternal age remains the best marker of oocyte/embryo developmental competence, which is the ability of an egg or embryo to generate a live birth [14].

Amyloid-like substances (ALS) underlie aging of many long-lived cells, such as neurons. Amyloids are elongated, unbranched proteins that generate a characteristic (cross-beta-sheet) diffraction pattern when exposed to x-rays [15]. An especially unique characteristic of these proteins is their ability to self-replicate and adapt to varying environments [16]. Since their discovery 150 years ago, they have been linked with necrosis and inflammation [17–20]. Their contributory role in several neurodegenerative diseases has been highlighted [21, 22]. Interestingly, besides their pathological role, ALS play functional roles in a number of organs [23], including melanin formation in skin and thyroid hormone storage in the thyroid gland [24–27]. They also have been described in the reproductive tract. In the epididymis and in the acrosome of mice spermatozoa, ALS play essential roles in sperm maturation. In follicular cells of frog oocytes, they facilitate cellular communication, and in oocytes, they contribute to the structure of the zona pellucida [28–31].

A recent study demonstrated that aggregates of ALS, widely known for its toxic effects in most cells, in budding yeast translationally repress cyclins and ensure homologous chromosome segregation and control gametogenesis. During meiosis I, Rim4, an RNA-binding protein that in vitro forms amyloid fibrils structures, inhibits the translation of cyclin type B (CLB3) and numerous other microRNAs, allowing proper separation of homologous chromosomes. Throughout the second meiotic division, Rim4 is degraded, granting the correct translation of CLB3 and proper conclusion of gamete cell division process [32].

Considering the potential of amyloid structures to become a future marker of oocyte function and quality and the lack of studies investigating their presence and distribution in mammalian oocytes and embryos, we sought to identify and characterize amyloid-like substance in oocytes, cleavage stage embryos, and blastocysts, using a murine model, and in immature and mature oocytes using a human model. We also aimed to evaluate the relationship between levels of amyloid in human oocytes and clinical characteristics of the patients submitted to ART treatment.

Materials and methods

Mouse samples

For a pilot study, we studied metaphase II mouse oocytes and in vivo fertilized embryos (1-cell, 2-cell, 4-cell, 8-cell, and blastocyst) ($n = 42$ samples for each stage) (Embryotech Laboratories, Inc., Wilmington, MA), which did not require approval from the Institutional Animal Committee. Each straw was removed from the liquid nitrogen container and left at room temperature for 2 min, then moved to a 37 °C water-heated container for another 1 min before cutting the straw and transferring the samples to a Petri dish containing M2 culture medium (EmbryoMax® M2 Medium (1×)). Half of the samples ($n = 126$) were used for immunofluorescence microscopy and the other half ($n = 126$) for electron microscopy.

Human samples

Patients were submitted to a controlled ovarian hyperstimulation cycle (COH) using gonadotropin-releasing hormone (GnRH) downregulation, microdose leuprolide acetate, or GnRH-antagonist protocols and exogenous gonadotropins (recombinant follicle-stimulating hormone (FSH) and human menopausal gonadotropin (hMG)). When lead follicles reached at least 18-mm mean diameter, final oocyte maturation was induced using a subcutaneous injection of Ovidrel, or leuprolide acetate. Oocyte retrieval via transvaginal ultrasound-guided needle aspiration of ovarian follicular fluid was performed 36 h later.

Immature oocytes were obtained according to the IRB approved study H6902. A total of 50 germinal vesicles (GV) and metaphase I (MI) human oocytes donated for research, from women ages 18–45, were collected. The first 10 to 15 oocytes were fixed within a few hours of retrieval and the remainder underwent in vitro maturation (IVM). GV oocytes were reevaluated regarding the nuclear maturation degree after 24 h of IVM and fixed at the Arrest GV or MI stages. MI oocytes were reevaluated after 24 h of IVM and fixed at the Arrested MI or MII stages. We adopted the terminology "Arrested" for oocytes that did not progress in their development after 24 h of IVM. All samples were fixed between 3 and 48 h after the retrieval. Four IVM MII oocytes were parthenogenetically activated. Only two of four successfully activated, resulting in one 2-cell and one 4-cell embryos. These two samples were fixed in a 2-cell and 4-cell embryo stages. All human samples were assigned to immunostaining.

We analyzed clinical variables including patient's age, weight and height, body mass index, history of smoking

tobacco, reproductive procedures, infertility diagnosis, anti-müllerian hormone (AMH) level before stimulation cycle, stimulation cycle length, type and dose of GnRH antagonist, type and dose of gonadotropin, stimulation protocol used, type and dose of trigger, estradiol on the day of trigger, total dose of gonadotropin, date and time of retrieval, number of eggs collected, number of eggs donated, time of the trigger, type of stimulation cycle (frozen or fresh), date/time and state of fixation, time between retrieval and fixation, and hours after trigger.

AMH levels were measured by the same assay (Quest Diagnostics Tests–CPT 82397) at clinical laboratories. AMH concentrations above and below 1.06 ng/ml were compared, because this level best differentiates response to ovarian stimulation, retrievable oocytes, and odds of live birth (Gleicher, 2010). Data were de-identified to ensure privacy.

Mouse parthenogenetic activation

Oocyte activation was induced chemically by exposure to 5 μM ionomycin in Global (G2) medium (Vitrolife, Göteborg, Sweden) for 5–10 min at 37 °C, to increase the oocyte's permeability to calcium and initiate a calcium release to trigger activation. This was followed by incubation in 1 mM 6-dimethylaminopyridine (6-DMAP) (Sigma) and 5 μg/ml cycloheximide (Sigma) in G2 medium for 3–4 h, under standard culture conditions (37 °C, 5% CO_2). 6-DMAP prevents the release of the second polar body under otherwise standard oocyte culture conditions, to create a diploid parthenote. After the activation process, eggs were placed singly in 50-μl drops of Global total (GT) medium under oil (Ovoil; Vitrolife). Oocytes were checked for the presence of pronuclei 6 h after activation. Successfully activated oocytes were transferred to fresh GT medium and cultured in 50-μl drops until day 5 or arrest, identified as 24 h without cleavage.

Immunofluorescence microscopy

Mouse and human samples were processed for indirect immunofluorescence. Chromosomes were stained with DAPI (4′, 6-diamidino-2-phenylindole; Cat. No. D1306). For detection of ALS, oocytes and embryos were fixed in freshly prepared 3.7% paraformaldehyde, permeabilized, incubated with Anti-Amyloid Fibril OC Antibody [AFOC] (1:1000, Millipore, AB2286), then labeled with a secondary fluorescence-labeled antibody. Samples were mounted in Vectashield mounting medium (Vector Laboratories, CA, USA).

A Zeiss AxioObserver with 20× Plan-Apochromat N.A. 0.8, narrow pass filter blocks for fluorescence, and an Axiocam 503 cooled CCD camera with 14 bits were used to image one picture of each field at constant illumination, exposure, and gain settings. These linear images were loaded into ImageJ, where each feature was traced, and the mean and integrated intensity were measured. The background was subtracted and plotted using GraphPad Prism 5.0. Z series were collected using a Zeiss 880 laser scanning confocal microscope with a 63× Plan-Apochromat N.A. 1.4 lens. For immunofluorescence, one to three images were taken for each sample. Images displayed using average pixel projection with linear contrast adjustment to show morphology. All samples were prepared simultaneously under identical conditions and then imaged together in a single session under identical conditions. As the 2-cell embryo stage was considered to be the brightest sample, each run of the experiment was normalized to the result at 2-cell embryo stage. However, with only two samples of parthenogenetic human embryos, quatatative analyses were not performed. Here, we adopted arbitrary units (a.u.) to report intensities, knowing that intensities are relative only within each set o images per imaging session assuming they were all stained and imaged under identical conditions.

Electron microscopy

Transmission electron microscopy was carried out in the Microscopy Core Laboratory at NYU Langone School of Medicine. Mouse oocyte, 1-cell, 2-cell, 4-cell, and 8-cell embryos, as well as blastocysts were isolated and washed twice in 0.1% PBS-PVP.

For morphology analysis, cells were fixed with 2.5% glutaraldehyde in PBS-PVP (pH 7.2) for 1 h and post-fixed with 1% osmium tetroxide for 1.5 h at room temperature, then processed in a standard manner, and embedded in LX112 resin (Electron Microscopy Sciences, Hatfield, PA). Semithin sections were cut at 500 nm and stained with 1% toluidine blue to evaluate the quality of preservation.Ultrathin sections (60 nm) were cut, mounted on copper grids, and stained with uranyl acetate and lead citrate by standard methods.

To localize ALS, we performed immunolabeling using both pre-embedding and Tokuyasu methods. For pre-embedding immunolabeling, cells were fixed with 3.7% paraformaldehyde in PBS for 15 min. After washing with PBS, cells were blocked with 3% goat serum, and 0.1% BSA for 30 min, then treated with 0.1% TritonX-100 in blocking buffer for 30 min. Cells were washed with blocking solution over 10 h at 4 °C and incubated with anti-amyloid fibril OC antibody (AFOC, Millipore) for 2 h at room temperature, then at 4 °C overnight. The cells were washed with blocking buffer, and nanogold conjugated secondary antibody (Nanoprobes, Yaphank, NY) was applied. After fixing with 1% glutaraldehyde in PBS for 5 min, silver enhancement (HQ Silver enhancement kit, Nanoprobes, Yaphank, NY) was performed in the dark for 8 min. Cells were washed with distilled water, fixed in 0.5% OsO4 for 15 min, counterstained with 0.5% uranyl acetate for 1 h at 4 °C, dehydrated in ethanol, and embedded in LX112. Ultrathin sections (60 nm) were cut,

mounted on copper grids, and stained with uranyl acetate and lead citrate by standard methods.

For the Tokuyasu method, cells were fixed with 2% paraformaldehyde in 0.1 M PBS-PVP containing 0.5% glutaraldehyde, pH 7.2–7.4 for 4 h at 4 C. Sucrose-infused tissues were cryosectioned at 80 nm and incubated with anti-amyloid fibril OC antibody, followed by application of colloidal gold conjugated protein A or goat anti-rabbit conjugated secondary antibodies (18 nm colloidal gold-affiniPure goat anti-rabbit IgG (H + L), Jackson Immuno Research Laboratories, Inc., West Grove, PA; 15 nm protein A gold, Cell Microscopy Center, University Medical Center Utrecht, 35584 CX Utrecht, The Netherlands) were applied and stained with methyl cellulose-uranyl acetate.

All stained grids were examined under a Philips CM-12 electron microscope and photographed with a Gatan (4 k × 2.7 k) digital camera. For electron microscopy, 12 to 19 pictures were taken for each sample.

Statistical analysis

SAS version 9.4 (SAS Institute) was used to perform data analyses. Descriptive statistics were calculated for all variables in the data set. Mean, standard deviation, and ranges were computed for continuous variables, while frequencies were calculated for categorical variables. Normally distributed data were compared by one-way analysis of variance (ANOVA), with the least square-MEANS post-test for group effects. Pearson correlation coefficients (r) were calculated to evaluate the relationships between continuous variables (e.g., number of oocytes retrieved and AMH level), depending on whether data were normally distributed. Univariate analyses (t tests and χ^2) were conducted to assess the relationships between all independent variables. Differences were considered to be statistically significant if $P < .05$.

Results

Mouse—immunofluorescence microscopy

In all 126 samples, immunostaining for ALS appeared throughout the cytoplasm and nucleus of oocytes and preimplantation embryos. From oocyte to 8-cell embryo stages, a significant amount of ALS was distributed homogeneously throughout the cytoplasm. In blastocyst stage embryos, a greater concentration of ALS appeared in the inner cell mass and trophoblast cells. The data suggest that ALS was excluded from some nuclei of the inner cell mass (Fig. 1a). Control specimens, in which the first antibody in the immunostaining process was omitted ($n = 10$ samples among different stages), exhibited no significant immuno staining (Fig. 1b).

Quantitative analysis showed high levels of ALS in oocytes (56232479.7 ± 5362949.38 a.u.) and 1-cell embryos (58544435.0 ± 7823810.44 a.u.), followed by sharply increased levels in 2-cell embryos (69000187.4 ± 6733098.07 a.u.). ALS reaches its lowest level in blastocysts (24423606.2 ± 4882808.37 a.u.) (Fig. 2). Levels of ALS differ across the various stages of development, with significant differences between oocyte and 2-cell embryos ($p < .0001$) and 2-cell embryos and blastocysts ($p < .0001$). ALS levels did not differ between oocyte and 1-cell embryos (56232479.7 ± 5362949.38 a.u. vs. 58544435.0 ± 7823810.44 a.u.; $p = 0.2715$) (Table 1).

Mouse—electron microscopy

Consistent with light microscopy results, ALS forms crystal sheet-like structures and protein aggregates inside the cytoplasm of all stage embryos, including blastocysts. Electron microscopy showed homogenous distribution of immune staining for ALS throughout the cytoplasm and nucleus of oocytes, 1-cell and 2-cell embryo stage. At the 4-cell embryo stage, ALS is more concentrated in some areas of the cytoplasm. These data suggest that ALS appeared in less quantity in the 8-cell and blastocyst stages (Fig. 3a). We also detected ALS in the autophagosomes of 8-cell stage embryos (Fig. 3b). No significant labeling appeared in control groups, in which the primary antibody had been omitted (Fig. 3b). In the literature, ALS in brain tissue in vivo analyzed by TEM have the same behavior demonstrated in our results. They form numerous diffuse plaques and clusters of dot and rod stains, very similar to our findings [33, 34].

Human—immunofluorescence microscopy

Fifty immature oocytes from 11 unique patients were accessioned for this study. Patient characteristics and ART techniques are shown in Table 2. Patients averaged 36 (± 2.94) years of age, none smoked, and mean body mass index was 24.19 (± 3.25) kg/m^2. Among eight patients submitted to in vitro fertilization (IVF), 27.5% had female factor, 58.8% male factor, and 13.7% had unexplained infertility. Two patients had elective egg freezing (EEF) cycles. AMH levels averaged 4.42 (± 2.13) ng/ml. Mean number of days of stimulation was 10.2 (± 0.85) days. The mean value of the estradiol on day of trigger was 3285 (± 1512) ng/dl, and total dose of gonadotropin used averaged 2958 (± 1249) IU. A total of 206 eggs were collected after retrievals, and 46 immature eggs were donated for our study. The time between retrieval and sample fixation averaged 7 h for fresh GV and MI and 27 h for arrested GV, MI, and MII oocytes. The time after the trigger averaged 42 h for fresh GV and MI and 63 h for arrested GV, MI, and MII oocytes.

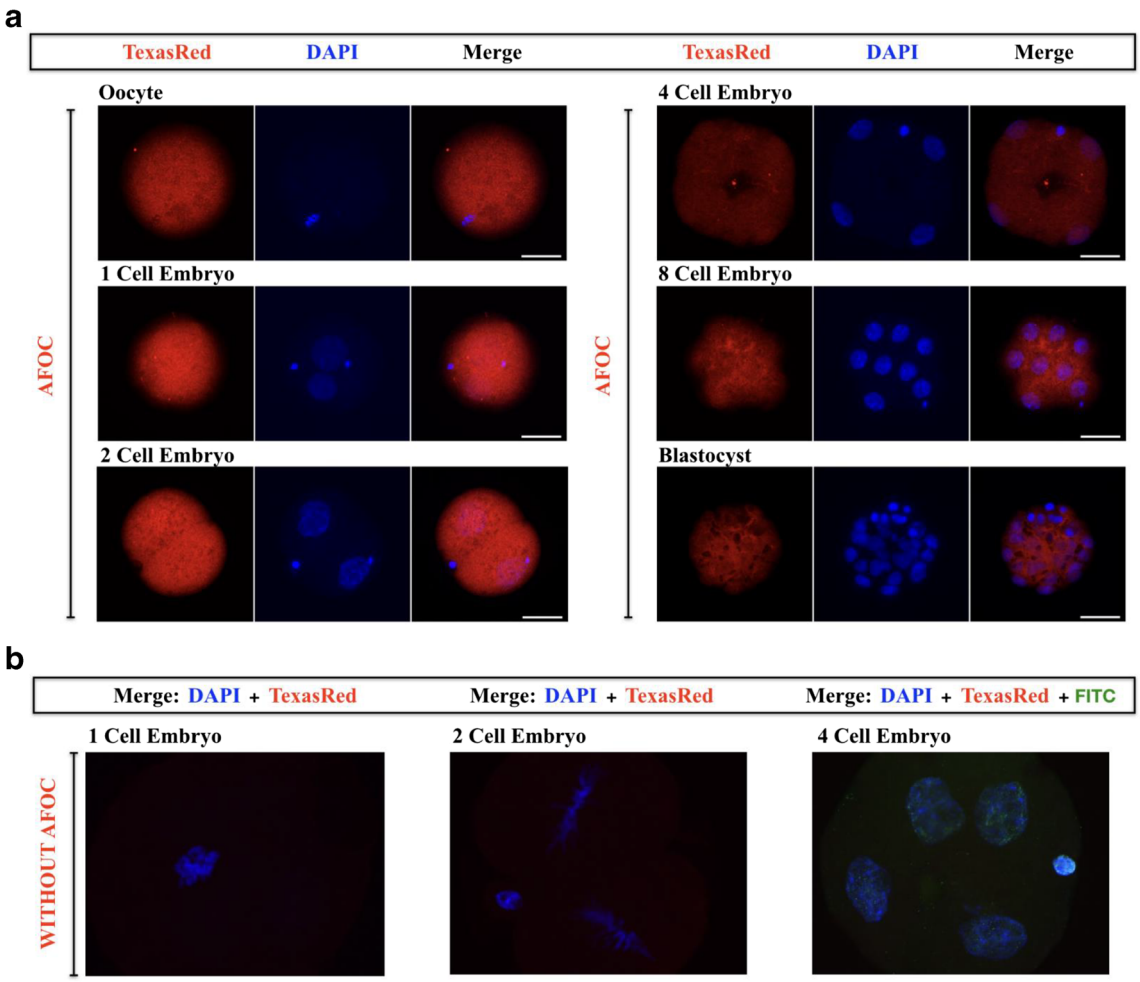

Fig. 1 Descriptive data of amyloid-like substance using immunostaining among mice oocytes and embryo stages. **a** Single-plane images of representative oocytes and embryos are shown with a scale bar of 5 μm. Amyloid-like substance forms static aggregates in cells. Cells were imaged starting at 3 h after fixation. Representative cells are shown with AFOC in red and the nucleus in blue. **b** Control specimens, in which the first antibody in the immunostaining process was omitted, exhibited no significant immuno staining. In the 4-cell embryo stage sample, we used another first antibody (anti-gamma H2A.X antibody [EP854(2)Y], with the secondary antibody FITC) as a positive control

In all 50 samples, immunostaining for ALS appears throughout the zona pellucida, as well as in the cytoplasm and nucleus of oocytes, polar bodies, and parthenogenetic embryos. In GV oocytes, a significant amount of ALS was distributed heterogeneously throughout the cytoplasm. Less staining and more heterogeneous distribution were identified in MI and MII oocytes. ALS was also indentified in 2-cell parthenogenetic embryo stage with heterogeneous distribution. The images seem to demonstrate reduced staining in 4-cell parthenogenetic embryo stage. No significant labeling appeared in control groups, in which the primary antibody had been omitted (Fig. 4).

Quantitative analysis showed that fresh GV oocytes possess higher levels (4164.74 ± 1573.46 a.u.) of ALS. This stage was followed by arrested GV (2967.67 ± 659.06 a.u.), fresh MI (2601.58 ± 1143.79 a.u.), MII (2495.25 ± 1775.88 a.u.), and arrested MI (2311.80 ± 986.36 a.u.) oocytes (Fig. 5). Using analysis of variance, there were significant differences of ALS between fresh GV and fresh MI (4164.74 ± 1573.46 a.u. vs. 2601.57 ± 1143.70 a.u.; $p = 0.008$) and fresh GV and MII (4164.74 ± 1573.46 a.u. vs. 2495.25 ± 1775.88 a.u.; $p = 0.008$) oocytes. There were no significant differences between fresh GV and arrested GV (4164.74 ± 1573.46 a.u. vs. 2967.66 ± 659.06 a.u.; $p = 0.079$) and fresh MI and arrested MI (2601.57 ± 1143.70 a.u. vs. 2311.80 ± 986.36 a.u.; $p = 0.705$) (Table 3).

To clarify the association between levels of ALS and clinical characteristics of patients submitted to IVF treatments, cycles were categorized in groups by age (< 35 vs. ≥ 35 years old), body mass index (< 25 vs. ≥ 25 kg/m^2), treatment modality (IVF vs. EEF), type of gonadotropin (follistim vs. gonal F), and stimulation cycle type (fresh vs. frozen). Higher levels of ALS were found in infertile patients submitted to IVF treatment compared to EEF (3335.6 ± 1736.5 a.u. vs. 2786.9 ± 1032.0 a.u.; $p = 0.032$) and in patients who used gonal F instead of follistim (3672.3 ± 1516.4 a.u. vs. 2017.9 ±

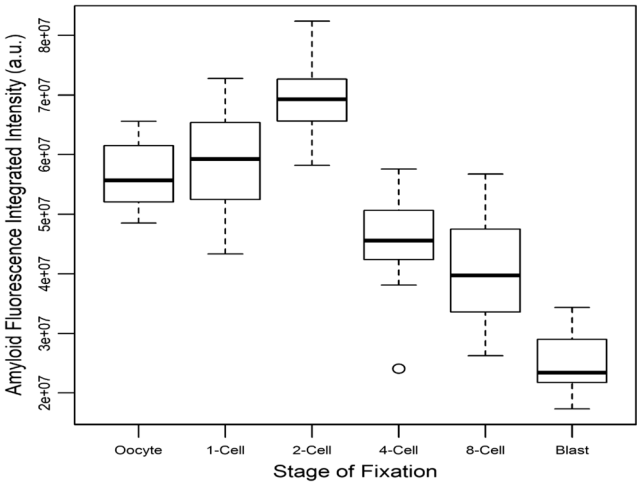

Fig. 2 Boxplot showing levels of amyloid-like substance by integrated intensity of immunostaining signal according to the stage of fixation in mice oocytes and embryo stages. Quantification of AFOC signal was established using Image J program

758.2 a.u.; $p = 0.008$) (data not shown). There were no significant differences of ALS levels between the age groups studied (4026.61 ± 1987.71 a.u. vs. 2998.77 ± 1427.13 a.u.; $p = 0.219$) and type of stimulation cycle (2912.8 ± 1311.30 a.u. vs. 4178.2 ± 2087.0 a.u.; $p = 0.062$) (data not shown). A significant negative correlation was found between levels of ALS and body mass index (− 0.54; $p = 0.0007$) (Fig. 6a), number of days of stimulation (− 0.44; $p = 0.002$) (Fig. 6b), dose of hMG (− 0.44; $p = 0.002$) (Fig. 6c), time between retrieval and fixation (− 0.33; $p = 0.023$) (Fig. 6d), and hours after trigger (− 0.33; $p = 0.023$) (Fig. 6e). There were no significant correlations between levels of ALS and age (0.06; $p = 0.667$), level of estradiol day of trigger (− 0.11; $p = 0.433$), total dose of gonadotropin (− 0.27; $p = 0.666$), and number of retrieved eggs (− 0.10; $p = 0.467$) (data not shown).

Some variables were categorized into three groups and levels of ALS compared to cause of infertility (female factor vs. male factor vs. unexplained), AMH level (< 1 ng/ml vs. 1–3 ng/ml vs. > 3 ng/ml), and type of GnRH analog (Antagon vs. Cetrotide vs. microdose lupron). Higher levels of ALS were found in patients undergoing IVF treatment for male factor compared to unexplained (3926.35 ± 1861.0 a.u. vs. 2550.47 ± 1222.1 a.u.; $p = 0.004$) (Fig. 7a). Significant differences also were found among AMH level categories, where higher levels of ALS were found in patients with AMH between 1 and 3 ng/ml when compared to < 1 ng/ml (4592.6 ± 2126.3 a.u. vs. 737.3 ± 14.7 a.u.; $p = 0.0002$) and > 3 ng/ml (4592.6 ± 2126.3 a.u. vs. 3197.2 ± 895.0 a.u.; $p = 0.006$) (Fig. 7b). Higher levels of ALS were found in patients that received Cetrotide compared to those receiving Antagon (3871.7 ± 1660.1 a.u. vs. 2368.5 ± 993.4 a.u.; $p = 0.0008$) (Fig. 7c). There was no significant association between levels of ALS and type of drug used on the trigger (data not shown).

All control samples, from which the first antibody was omitted, did not specifically label any structures.

Discussion

Here, we first show that ALS, conventionally considered to have toxic and degenerative roles, is present in mammalian oocytes and embryos at levels which vary according to stage of development. We demonstrate that ALS is present in the

Table 1 Mean intensity of amyloid comparison among different groups in mice samples

Group	Mean intensity ± SD (a.u.)	Mean intensity ± SD (a.u.)	*p* value*
Oocyte vs. 1-cell	56232479.7 ± 5362949.38	58544435.0 ± 7823810.44	0.2715
Oocyte vs. 2-cell	56232479.7 ± 5362949.38	69000187.4 ± 6733098.07	< .0001
Oocyte vs. 4-cell	56232479.7 ± 5362949.38	45821432.8 ± 7155402.87	< .0001
Oocyte vs. 8-cell	56232479.7 ± 5362949.38	40071588.0 ± 8553533.04	< .0001
Oocyte vs. blastocyst	56232479.7 ± 5362949.38	24423606.2 ± 4882808.37	< .0001
1-cell vs. 2-cell	58544435.0 ± 7823810.44	69000187.4 ± 6733098.07	< .0001
1-cell vs. 4-cell	58544435.0 ± 7823810.44	45821432.8 ± 7155402.87	< .0001
1-cell vs. 8-cell	58544435.0 ± 7823810.44	40071588.0 ± 8553533.04	< .0001
1-cell vs. blastocyst	58544435.0 ± 7823810.44	24423606.2 ± 4882808.37	< .0001
2-cell vs. 4-cell	69000187.4 ± 6733098.07	45821432.8 ± 7155402.87	< .0001
2-cell vs. 8-cell	69000187.4 ± 6733098.07	40071588.0 ± 8553533.04	< .0001
2-cell vs. blastocyst	69000187.4 ± 6733098.07	24423606.2 ± 4882808.37	< .0001
4-cell vs. 8-cell	45821432.8 ± 7155402.87	40071588.0 ± 8553533.04	0.0067
4-cell vs. blastocyst	45821432.8 ± 7155402.87	24423606.2 ± 4882808.37	< .0001
8-cell vs. blastocyst	40071588.0 ± 8553533.04	24423606.2 ± 4882808.37	< .0001

Data are expressed as mean ± SD in each group

*p value related to the post-test LS-means (ANOVA)

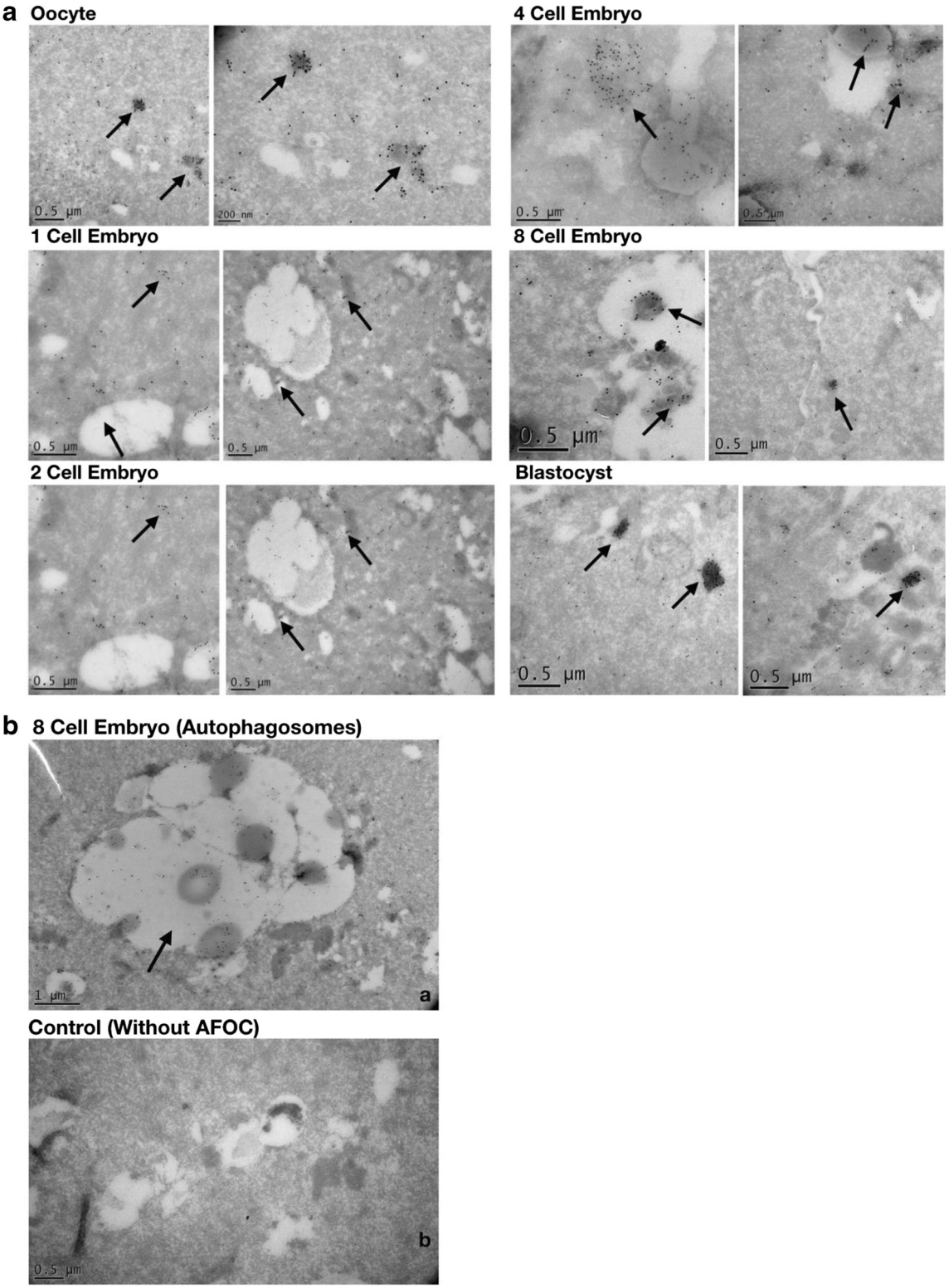

Fig. 3 Distribution of amyloid-like substance among mice oocytes and embryo stages illustrated by immunoelectron microscopy. Gold particles are labeled on protein aggregates (arrows at **a**) and inside autophagosome (**b**). There is no labeling on secondary antibody control (**b**) (the bar is the same for **a** and **b**, except oocyte and autophagosome)

nucleus and cytoplasm of mice oocytes and embryos and differ among the various stages of embryo development, with higher concentrations in early embryo stages. On the basis of these results, we speculate that ALS may play an important

Table 2 Clinical characteristics of patients

Characteristic	Mean	Std Dev (±)	*N*	(%)
Age (years)	36.65	2.95		
BMI (kg/m^2)	24.20	3.25		
AMH (ng/ml)	4.43	2.13		
Cause of infertility				
Female factor			8	17.39
Male factor			17	36.96
Unexplained			21	45.65
Treatment				
IVF			29	63.04
EEF			17	36.96
Type of cycle				
Fresh			38	82.61
Frozen			8	17.39
Days of stimulation	10.26	0.85		
E2 trigger day (ng/dl)	3285.30	1511.53		
Total dose gonadot (UI)	2957.61	1248.96		
Analog GnRH (no. patients)				
Antagon			20	43.38
Cetrotide			23	50.00
MDL			3	6.52
FSH (no. patients)				
Follist			15	32.61
Gonal F			31	67.39
Number of eggs	25.22	12.37		
Time Ret/Fix (min)	995.07	649.64		
Time after trigger (min)	3116.84	1525.33		
Stage of fixation				
Fresh GV			16	34.78
Arrested GV			6	13.04
Fresh MI			10	21.73
Arrested MI			6	13.04
Fresh MII			8	17.39

Data are expressed as mean ± SD or as percentage

BMI body mass index, *AMH* anti-müllerian hormone, *IVF* in vitro fertilization, *EEF* elective egg freezing, *E2* estradiol, *Gonadot* gonadotrophin, *FSH* follice-stimulating hormone, *Ret* retrieval, *Fix* fixation

role during embryo development. In budding yeast, it is involved in oocyte maturation and cell division. Considering our results that levels of ALS are high at the GV stage, we speculate that it may also play a role in oocyte maturation, especially at the conclusion of the first meiosis in mammalian oocytes. Our study also shows correlation between levels of ALS and good prognoses clinical characteristics in patients undergoing IVF treatments, such as normal BMI, adequate levels of AMH, and short controlled ovarian stimulation cycles. It will be interesting to determine whether ALS is associated with success rates during fertility treatment.

Recently, several studies have been conducted in order to better understand the complex molecular composition of the mammalian oocyte. Using transcriptional profiling and proteomics, Yurttas et al. concluded that the mature oocyte transcribes and stores a significant amount of substances, which, contrary to what was thought previously, are not used during oogenesis, but rather are required to regulate embryogenesis. These structures are considered essential for appropriate oocyte-to-embryo transition [35]. Intriguingly, mice oocytes, at around 2.5 weeks, begin intense metabolic activity, reflecting increased synthesis of mRNAs and proteins. However, most of these structures are stored in the oocyte for use after fertilization [36]. The exact mechanism of storage of these molecules is not yet fully understood, but many molecules take the form of ALS to achieve efficient storage, e.g., in thyroid, where peptide and protein hormones are stored in secretory granules in amyloid-like aggregations [27]. Presumably, some mRNAs and proteins can be stored in amyloid-like configurations until early stages of development, particularly up to the 2-cell embryo stage. Our findings that levels of ALS peak in mature oocytes and 2-cell embryos are consistent with such a storage role for ALS.

Another interesting point is that the different distribution of ALS among various stages is consistent with a possible regulatory function during early embryonic development. One of the major milestones of the oocyte-embryonic transition is the zygotic gene activation (ZGA), when the development program governed by maternally inherited proteins and transcripts is replaced by a new program commanded by the expression of new genes [37]. Three main changes that occur during this period are essential to the correct embryo development. First, there must be a destruction of oocyte-specific transcripts, which is followed by the replacement of maternal transcripts by zygotic transcripts and finally a complete gene expression reprogramming [38, 39]. In mice, the most critical transformation starts at the 1-cell embryo stage, when transcription from the male pronucleus begins [40]. Although the process starts at this stage, complete synchronization between transcription and translation occurs only at the 2-cell embryo stage. Therefore, genome activation actually occurs at the 2-cell embryo stage, when the zygotic nuclei are formed, and genes are rapidly expressed [41]. Another important mechanism that is critical at the 2-cell stage is the embryo epigenetic reprogramming mechanism, which is responsible for regulating gene activity without altering the primary DNA sequence and becoming inheritable throughout the cell divisions. In mammals, DNA methylation constitutes one of the most stable epigenetic modifications and studies have shown that these DNA methylation patterns directly influence the embryo development. In mouse, the paternal genome undergoes an active demethylation immediately after fertilization, while in the maternal genome this reduction occurs only after the 2-cell embryo stage, showing that somehow, the

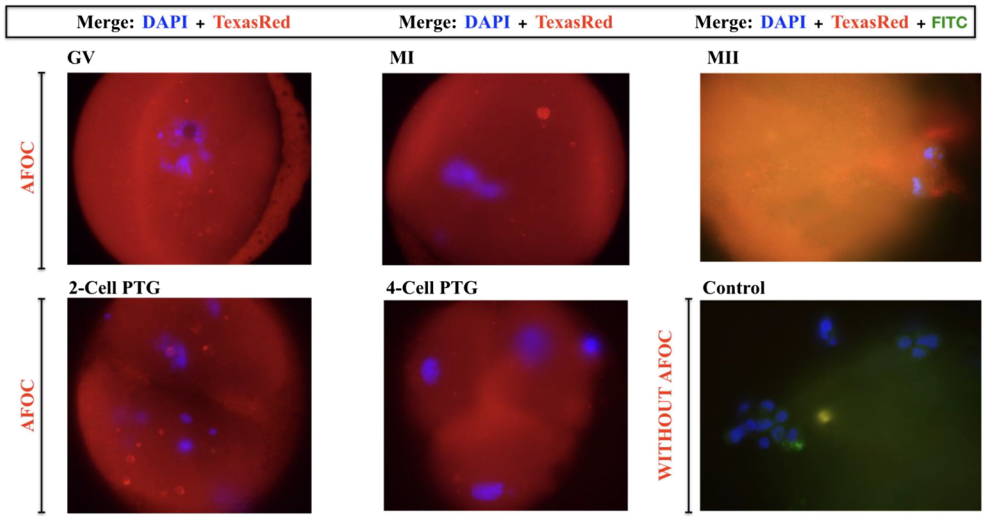

Fig. 4 Descriptive data of amyloid-like substance using immunostaining among human immature and in vitro mature oocytes, and parthenogenetic embryos. Single-plane images of representative single cells are shown. Scale bar, 5 μm. Amyloid-like substance forms static aggregates in cells. Cells were imaged starting at 3 h after fixation. Representative cells are shown with AFOC in red and the nucleus in blue. Control specimens, in which the first antibody in the immunostaining process was omitted, exhibited no significant immuno staining. In the MII and control samples, we used another first antibody (anti-gamma H2A.X antibody [EP854(2)Y], with the secondary antibody FITC) as a positive control

maternal genome is protected until the embryo reaches this stage [42]. In the next stage of development, the 4-cell embryo stage, approximately 45% of genes are repressed, a stage known as the transcriptionally repressive state. Transcriptional repression is controlled by histone methylation [43]. These observations suggest that the appearance of ALS at earlier stages of development may not be an accident. Conceivably, ALS might be involved in the zygote transcription and translation processes and in the embryo epigenetic reprogramming mechanism, since higher levels of ALS were found in the 1- and 2-cell stage embryos. From the 4-cell embryo stage, with the onset of the transcriptionally repressive state, when many genes are suppressed, levels of ALS begin to fall.

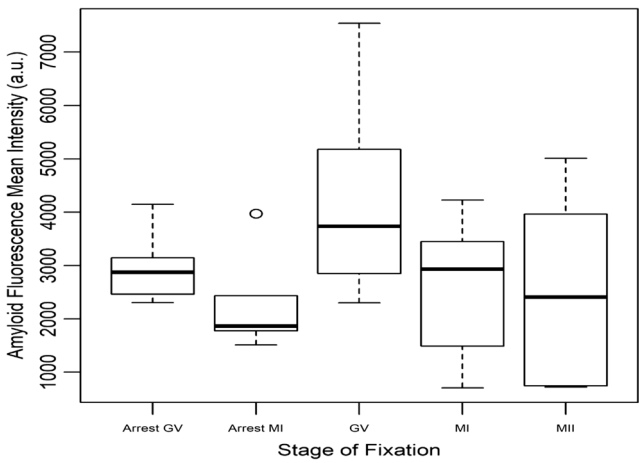

Fig. 5 Boxplot showing levels of amyloid-like substance by mean intensity of immunostaining signal according to the stage of fixation in human immature and mature oocytes. Quantification of AFOC signal was established using Image J program

It has been shown that in fertilized embryos, zygote RNA production was repressed in the 2-cell embryo stage, but in the case of parthenogenetic activated embryos, this phenomenon was maintained until the 4-cell embryo stage, confirming a delay in the zygote RNA repression in parthenogenetic embryos [44]. The lack of the paternal genome may contribute to this abnormality, as data suggest that the paternal genome may be involved in the activation of the embryonic genome [40]. Our results show that even in the paternal genome absence, immunostaining for ALS was positive in the two human parthenogenetic activation samples. This finding reinforces our hypothesis that ALS may be part of the group of maternal provided proteins and transcripts that are degraded and silenced throughout embryonic development, from the moment that the embryonic genome activation begins. Analyzing only the qualitative results, it appears that the amyloid signal remains high in the parthenogenetic 4-cell embryo stage, reinforcing the aforementioned study where the authors note a delay in the transcriptional repression state in those embryos that do not have the paternal genome influence.

Studies have shown that the male components of the zygote, such as sperm mitochondria, the microtubule-organizing center precursors, and the cellular components from the sperm, play little role in cleavage-stage embryogenesis [45]. Therefore, early stage embryos are entirely dependent on the oocyte molecules and organelles for their survival, until activation of the embryonic genome at cleavage stage of development [46]. By the 4- to 8-cell stages, degradation of maternal RNA and proteins is nearly complete [47]. This depletion is essential for embryonic development, since mutant mouse embryos, lacking this mechanism, do not progress beyond the 4- to 8-cell stage of development [48]. In our findings, levels

Table 3 Mean intensity of amyloid comparison among different groups in human samples

Group	Mean intensity ± SD (a.u.)	Mean intensity ± SD (a.u.)	*p* value*
GV vs. arrested GV	4164.74 ± 1573.46	2967.67 ± 659.06	0.0791
GV vs. MI	4164.74 ± 1573.46	2601.58 ± 1143.79	0.0080
GV vs. arrested MI	4164.74 ± 1573.46	2311.80 ± 986.36	0.0128
GV vs. MII	4164.74 ± 1573.46	2495.25 ± 1775.88	0.0083
MI vs. arrested GV	2601.58 ± 1143.79	2967.67 ± 659.06	0.6123
MI vs. arrested MI	2601.58 ± 1143.79	2311.80 ± 986.36	0.7051
MI vs. MII	2601.58 ± 1143.79	2495.25 ± 1775.88	0.8725
MII vs. arrested GV	2495.25 ± 1775.88	2967.67 ± 659.06	0.5321
MII vs. arrested MI	2495.25 ± 1775.88	2311.80 ± 986.36	0.8178

Data are expressed as mean ± SD in each group

*p value related to the post-test LS-means (ANOVA)

of ALS fall precisely from the 4-cell stage, reaching the lowest level at blastocyst stage. These findings were subsequently confirmed by electron microscopy. Eight-cell embryos have some ALS, but primarily within autophagosomes, which is the organelle responsible for cleaning proteins and transcripts that are no longer used. This is consistent with ALS having a more critical role during early rather than late embryo stages.

The process of oocyte maturation, which is closely related to the acquisition of oocyte competence, requires perfect synchronization between nuclear and cytoplasmic maturation. It involves not only the correct mechanism of homologous chromosome segregation, but also correct distribution of cytoplasmic organelles and stores of mRNA, proteins, and transcription factors [49]. Intra- and intercellular molecular changes are also involved in this mechanism, such as modification of chromatin configuration, changes in mitochondrial distribution, endoplasmic reticulum reorganization, and intracellular calcium channel signaling [50]. When the peak of luteinizing hormone (LH) occurs, grown oocyte in the stage of GV resumes meiosis I. At this phase, considered to be of extreme importance, the process of oocyte maturation intensifies before reaching the MII stage. Coincidently, in human immature oocytes at the GV stage, we found a higher concentration of ALS, corroborating findings by Berchowitz et al., where, in yeast, prophase I stage possesses the highest level of ALS, which controls meiosis at this point. An amyloid-like protein, called Rim4, represses the translation of numerous mRNAs until the onset of meiosis II. At the MII stage, Rim4 is fully degraded, allowing the mRNA CLB3 transcription and completion of meiosis [32]. In our study, the lowest levels of ALS were found at the MII stage. Our results suggest that in humans, ALS may be involved in completion of meiosis I. Future studies should examine whether it can serve as a biomarker of oocyte quality.

The study mentioned above is conducted in budding yeast and investigates the interaction of ALS with cyclin B3. Coincidentally, in mammalian oocytes, the arrest and consumption of meiosis are also mainly controlled by phosphorylation and dephosphorylation of cyclin-dependent kinases (Cdks) [51]. A near correlation between cyclins and amyloid substance was published using human neurons as a model. In previous reports, dominant negative forms of Cdk4, Cdk2, and Cdk6 prevented amyloid-induced neuronal death, protecting neurons against amyloid toxicity [52, 53]. In a recent study, they also showed that Cdk inhibitors could efficiently block the cellular toxicity elicited by amyloid proteins, partly rescuing and delaying the neuronal apoptosis [54]. Since oocytes and neurons care out some similarities such as the fact that they are already differentiated cells without regeneration potential, we believe that the interaction between ALS and cyclins might be involved in controlling oocyte maturation mechanism.

A correlation between levels of ALS in follicular fluid and IVF outcome previously has been described by Duan et al. [55]. In follicular fluid of infertile women undergoing IVF, the proteolysis product of amyloid precursor protein, Aß40, was significantly higher in patients who achieved pregnancy (n = 26; 50.98%) compared to those with unsuccessful cycles (n = 25; 49.02%; p = 0.024). They also found a positive correlation between levels of Aβ40 and number of antral follicles (R = 0.407, p = 0.000) and oocytes retrieved (R = 0.476, p = 0.000). In the same study, granulosa cells from mice treated with amyloid substance showed better proliferation capacity and better expression of key molecules involved in steroidogenesis, such as IGF-1, FSH-receptor, and P450 aromatase, concluding that adequate level of amyloid is important for embryo development. These results are consistent with those in our study, where higher levels of ALS were found in good prognosis patients undergoing IVF, such as normal body mass index, brief controlled ovarian stimulation, AMH level between 1 and 3 ng/ml, and diagnosis of male or unexplained factor.

Another interesting finding was described by Urieli-Shoval et al. [56]. Levels of serum amyloid A(SAA), a

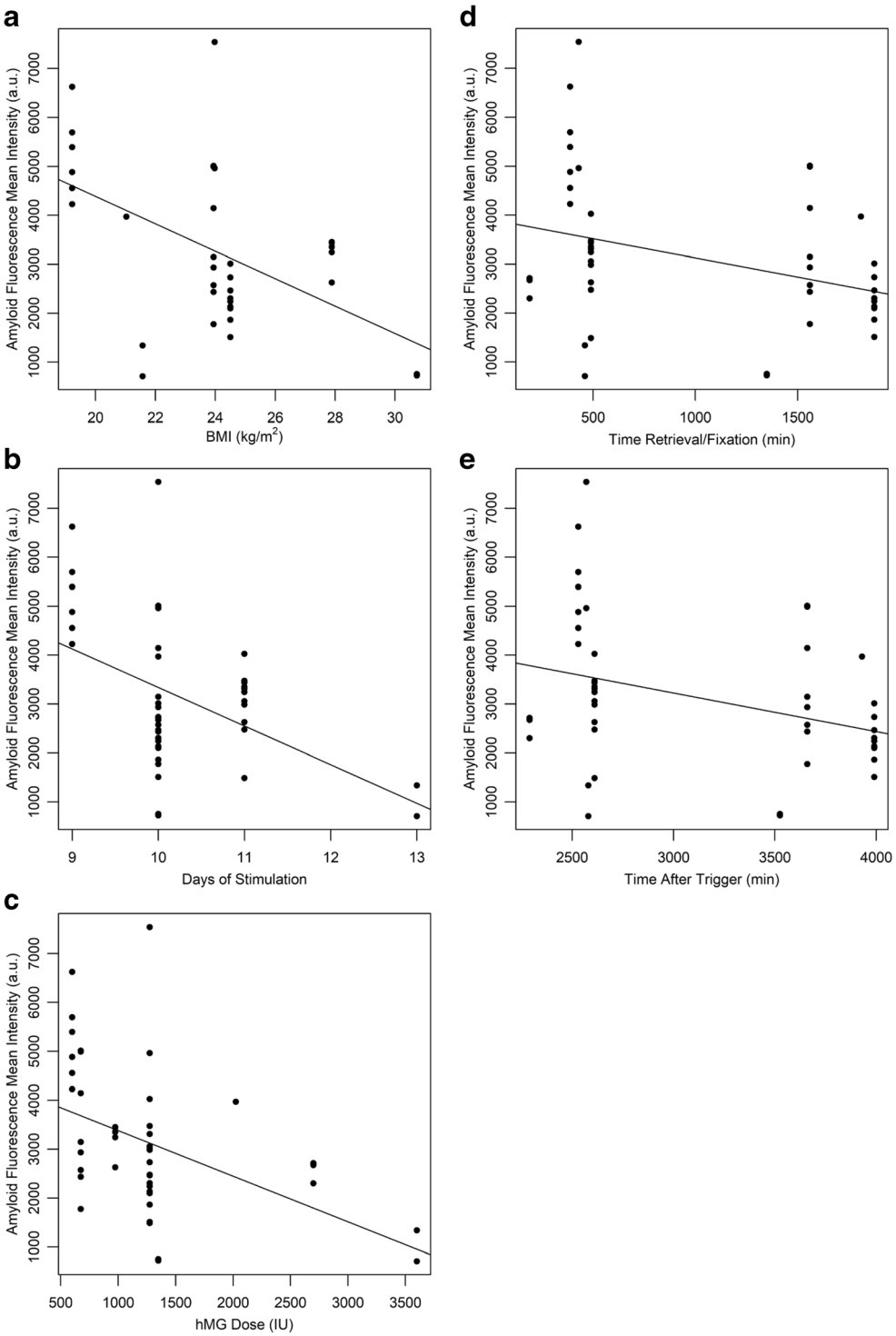

Fig. 6 **a** Negative linear correlation between levels of amyloid, measured by mean intensity, and BMI (Pearson correlation coefficients 0.54097; $p = 0.0007$). **b** Negative linear correlation between levels of amyloid, measured by mean intensity and days of stimulation (Pearson correlation coefficients 0.44136; $p = 0.0021$). **c** Negative linear correlation between levels of amyloid, measured by mean intensity, and hMG dose (Pearson correlation coefficients 0.44208; $p = 0.0021$). **d** Negative linear correlation between levels of amyloid, measured by mean intensity, and time between retrieval and fixation (Pearson correlation coefficients 0.33304; $p = 0.0237$). **e** Negative linear correlation between levels of amyloid, measured by mean intensity, and time after trigger (Pearson correlation coefficients 0.33420; $p = 0.0232$)

different type of amyloid protein related to inflammatory processes, such as tissue injury, infection, and neoplasia, were measured in follicular fluid aspirates and blood samples from infertile women undergoing controlled ovarian stimulation cycles. Interestingly, the group of women who presented higher concentrations of SAA had a 50% reduction in pregnancy rate and had the highest age and body mass index. All these findings suggest that levels of ALS can influence IVF results.

In regard to the mice samples, this study was cross-sectional, so we can only infer that changes in ALS across development are taking place. As the embryos used were not cultured, we can only infer the change in amyloid levels rather than track changes over time. Further, as this

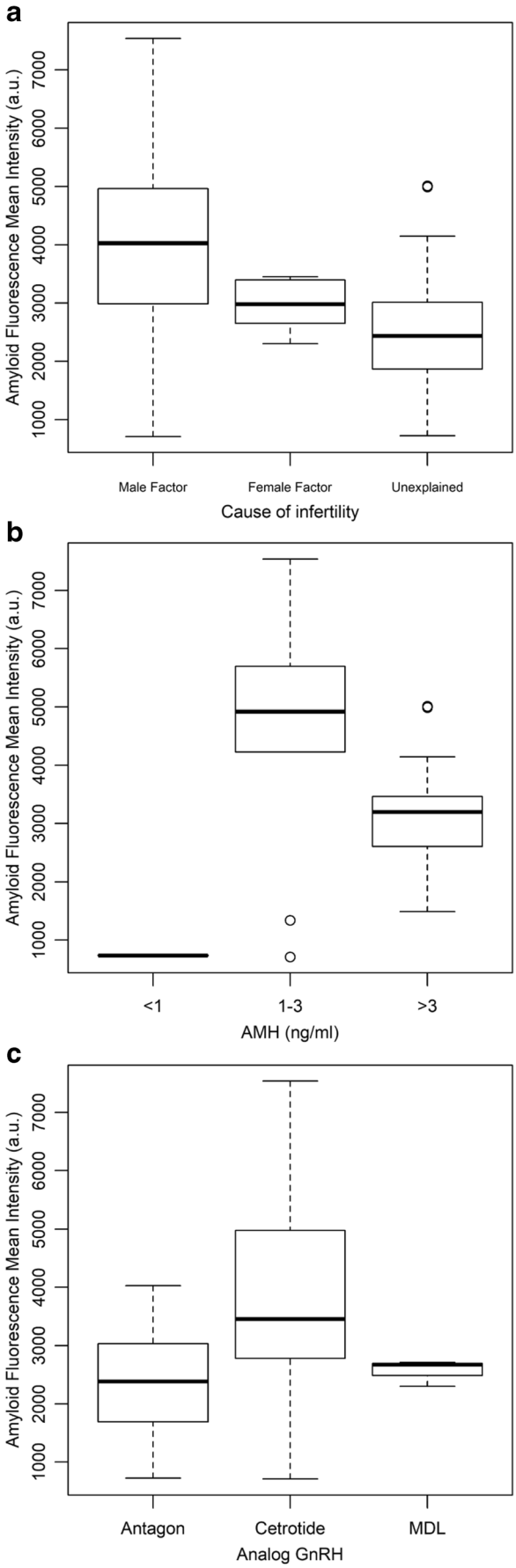

◀ **Fig. 7** **a** Boxplot showing the comparison of amyloid levels between "Cause of infertility" categories. Higher levels of amyloid were found in patients submitted to IVF for male factors when compared to unexplained cause (3926.35259 ± 1861.00 vs. 2550.47619 ± 1222.10; $p = 0.0049$). p values related to the post-test LS-means (ANOVA). **b** Boxplot showing the comparison of amyloid levels between AMH categories. Levels of amyloid was higher in the group of AMH between 1 and 3 ng/ml, when compared to < 1 ng/ml (4592.6 ± 2126.3 vs. 737.3 ± 14.7; $p = 0.0002$) and > 3 ng/ml (4592.6 ± 2126.3 vs. 3197.2 ± 895.0; $p = 0.0067$). p values related to the post-test LS-means (ANOVA). **c** Boxplot showing the comparison of amyloid levels between "type of Analog GnRH" categories. Higher levels of amyloid were found in patients who used Cetrotide instead of Antagon (3871.74643 ± 1660.09 vs. 2368.57185 ± 993.40; $p = 0.0008$). p values related to the post-test LS-means (ANOVA)

was a preliminary study, we have not performed functional assays to interrogate the functions of ALS in mouse oocytes and embryos. Today, methods used to identify and measure ALS are invasive and involve oocyte destruction, but in the future, as technology advances and the ability to screen oocytes in a noninvasive manner become possible, we will have the capacity to realistically improve the clinical outcomes of our infertility patients using the ALS levels.

The importance of the amyloid substance in the reproductive scenario may be greater than previously speculated. In xenopus and zebrafish oocytes, a subcellular compartment in the cytoplasm formed by amyloid configuration, known as Balbiani body, may be responsible for the conservative mechanism that helps oocytes function as long-lived germ cells [57]. This theory is substantiated by the fact that this amyloid structure only appears in oocytes at this dormancy state, behaving like a reversible functional amyloid, which at the slightest sign of oocyte activation ceases to exert its function and disappears [58]. Considering that amyloid could be a conserved evolutionary mechanism related to the oocyte quality and survival, we strongly belive that amyloid should be investigated further in the context ofreproduction.

No previous studies have investigated the expression and localization of ALS in mammalian oocytes and preimplantation embryos, so this work serves as the first to identify and quantify ALS in mammalian germ cells. We demonstrate, using two different methodologies, that levels of ALS vary across mouse development and peak in embryos at the 2-cell stage. We also show the presence and distribution of immunostaining for an ALS in immature and mature human oocytes and find that its level correlates with a number of good prognosis clinical characteristics. Since ALS can produce age-related cellular pathology, futures studies should investigate the role of ALS in oocyte aging and potential roles in female infertility, characterizing the physiological and/or pathophysiological roles of ALS during early development.

Conclusion

Whether in natural pregnancy or assisted reproduction techniques, female fertility reaches a biological limit, and the major culprit of reproductive aging is the female gamete. A marker of oocyte quality would enhance the selection of developmentally competent embryos. Due to the biological and pathological significance of ALS, and its presence in mammalian oocytes and embryos, future studies should address its role in embryo development.

Acknowledgements We thank NYULMC DART Microscopy Lab for their assistance: Alice Liang, Chris Petzold and K isten Dancel-Manning with TEM work, and Michael Cammer for LM work.

Compliance with ethical standards

Financial disclosure Support from FAPESP, Brazil (Process 2015/21907-0) (PN) and the Stanley H. Kaplan Endowment Fund.

References

1. Pastore LM, Christianson MS, Stelling J, Kearns WG, Segars JH. Reproductive ovarian testing and the alphabet soup of diagnoses: DOR, POI, POF, POR, and FOR. J Assist Reprod Genet. 2018;35(1):17–23.
2. Adhikari D, Zheng W, Shen Y, et al. Tsc/mTORC1 signaling in oocytes governs the quiescence and activation of primordial follicles. Hum Mol Genet. 2010;19:397–410.
3. Zhang H, Liu K. Cellular and molecular regulation of the activation of mammalian primordial follicles: somatic cells initiate follicle activation in adulthood. Hum Reprod Update. 2015;21(6):779–86.
4. Sun X, Su Y, He Y, Zhang J, Liu W, Zhang H, et al. New strategy for in vitro activation of primordial follicles with mTOR and PI3K stimulators. Cell Cycle. 2015;14(5):721–31.
5. Optimizing natural fertility. Fertil Steril. 2008;90(5 Suppl):S1–6.
6. Hornstein MD. State of the ART: assisted reproductive Technologies in the United States. Reprod Sci. 2016;23(12): 1630–3.
7. Takahashi T, Igarashi H, Amita M, Hara S, Matsuo K, Kurachi H. Molecular mechanism of poor embryo development in postovulatory aged oocytes: mini review. J Obstet Gynaecol Res. 2013;39(10):1431–9.
8. Broekmans FJ, Kwee J, Hendriks DJ, Mol BW, Lambalk CB. A systematic review of tests predicting ovarian reserve and IVF outcome. Hum Reprod Update. 2006;12(6):685–718.
9. Hassold T, Hunt P. To err (meiotically) is human: the genesis of human aneuploidy. Nat Rev Genet. 2001;2(4):280–91.
10. Battaglia DE, Goodwin P, Klein NA, Soules MR. Influence of maternal age on meiotic spindle assembly in oocytes from naturally cycling women. Hum Reprod. 1996;11(10):2217–22.
11. Keefe DL, Niven-Fairchild T, Powell S, Buradagunta S. Mitochondrial deoxyribonucleic acid deletions in oocytes and reproductive aging in women. Fertil Steril. 1995;64(3):577–83.
12. Polani PE, Crolla JA. A test of the production line hypothesis of mammalian oogenesis. Hum Genet. 1991;88(1):64–70.
13. Liu L, Keefe DL. Nuclear origin of aging-associated meiotic defects in senescence-accelerated mice. Biol Reprod. 2004;71(5):1724–9.
14. Scheffer JB, Scheffer BB, de Carvalho RF, Rodrigues J, Grynberg M, Mendez Lozano DH. Age as apredictor of embryo quality regardless of the quantitative ovarian response. Int J Fertil Steril. 2017;11(1):40–6.
15. Shewmaker F, McGlinchey RP, Wickner RB. Structural insights into functional and pathological amyloid. J Biol Chem. 2011;286(19):16533–40.
16. Riek R, Eisenberg DS. The activities of amyloids from a structural perspective. Nature. 2016;539(7628):227–35.
17. Li J, McQuade T, Siemer AB, Napetschnig J, Moriwaki K, Hsiao YS, et al. The RIP1/RIP3 necrosome forms a functional amyloid signaling complex required for programmed necrosis. Cell. 2012;150(2):339–50.
18. Loo DT, Copani A, Pike CJ, Whittemore ER, Walencewicz AJ, Cotman CW. Apoptosis is induced by beta-amyloid in cultured central nervous system neurons. Proc Natl Acad Sci U S A. 1993;90(17):7951–5.
19. Thomas T, Thomas G, McLendon C, Sutton T, Mullan M. Beta-amyloid-mediated vasoactivity and vascular endothelial damage. Nature. 1996;380(6570):168–71.
20. Akiyama H, Barger S, Barnum S, Bradt B, Bauer J, Cole GM, et al. Inflammation and Alzheimer's disease. Neurobiol Aging. 2000;21(3):383–421.
21. Pinzer BR, Cacquevel M, Modregger P, McDonald SA, Bensadoun JC, Thuering T, et al. Imaging brain amyloid deposition using grating-based differential phase contrast tomography. Neuroimage. 2012;61(4):1336–46.
22. Knowles TP, Vendruscolo M, Dobson CM. The amyloid state and its association with protein misfolding diseases. Nat Rev Mol Cell Biol. 2014;15(6):384–96.
23. Fowler DM, Koulov AV, Balch WE, Kelly JW. Functional amyloid–from bacteria to humans. Trends Biochem Sci. 2007;32(5):217–24.
24. Chapman MR, Robinson LS, Pinkner JS, Roth R, Heuser J, Hammar M, et al. Role of Escherichia coli curli operons in directing amyloid fiber formation. Science. 2002;295(5556):851–5.
25. Kwan AH, Winefield RD, Sunde M, et al. Structural basis for rodlet assembly in fungal hydrophobins. Proc Natl Acad Sci U S A. 2006;103(10):3621–6.
26. Fowler DM, Koulov AV, Alory-Jost C, Marks MS, Balch WE, Kelly JW. Functional amyloid formation within mammalian tissue. PLoS Biol. 2006;4(1):e6.
27. Maji SK, Perrin MH, Sawaya MR, Jessberger S, Vadodaria K, Rissman RA, et al. Functional amyloids as natural storage of peptide hormones in pituitary secretory granules. Science. 2009;325(5938):328–32.
28. Whelly S, Johnson S, Powell J, Borchardt C, Hastert MC, Cornwall GA. Nonpathological extracellular amyloid is present during normal epididymal sperm maturation. PLoS One. 2012;7(5):e36394.
29. Guyonnet B, Egge N, Cornwall GA. Functional amyloids in the mouse sperm acrosome. Mol Cell Biol. 2014;34(14):2624–34.
30. Parodi J, Ochoa-de la Paz L, Miledi R, Martinez-Torres A. Functional and structural effects of amyloid-beta aggregate on Xenopus laevis oocytes. Mol Cell. 2012;34(4):349–55.
31. Egge N, Muthusubramanian A, Cornwall GA. Amyloid properties of the mouse egg zona pellucida. PLoS One. 2015;10(6):e0129907.
32. Berchowitz LE, Kabachinski G, Walker MR, Carlile TM, Gilbert WV, Schwartz TU, et al. Regulated formation of an amyloid-like translational repressor governs gametogenesis. Cell. 2015;163(2): 406–18.
33. Chandra A, Copen CE, Stephen EH. Infertility and impaired fecundity in the United States, 1982–2010: data from the National Survey of Family Growth. Natl Health Stat Rep. 2013;(67):1–18 1 p following 19.
34. Al-Hilaly YK, et al. A central role for dityrosine crosslinking of amyloid-beta in Alzheimer's disease. Acta Neuropathol Commun. 2013;1:83.

35. Yurttas P, Morency E, Coonrod SA. Use of proteomics to identify highly abundant maternal factors that drive the egg-to-embryo transition. Reproduction. 2010;139(5):809–23.
36. Nothias JY, Miranda M, DePamphilis ML. Uncoupling of transcription and translation during zygotic gene activation in the mouse. EMBO J. 1996;15(20):5715–25.
37. Schultz RM. The molecular foundations of the maternal to zygotic transition in the preimplantation embryo. Hum Reprod Update. 2002;8(4):323–31.
38. Yu J, Hecht NB, Schultz RM. Expression of MSY2 in mouse oocytes and preimplantation embryos. Biol Reprod. 2001;65(4):1260–70.
39. Latham KE, Garrels JI, Chang C, Solter D. Quantitative analysis of protein synthesis in mouse embryos. I. Extensive reprogramming at the one- and two-cell stages. Development. 1991;112(4):921–32.
40. Aoki F, Worrad DM, Schultz RM. Regulation of transcriptional activity during the first and second cell cycles in the preimplantation mouse embryo. Dev Biol. 1997;181(2):296–307.
41. Schultz RM. Regulation of zygotic gene activation in the mouse. Bioessays. 1993;15(8):531–8.
42. Mann MR, Bartolomei MS. Epigenetic reprogramming in the mammalian embryo: struggle of the clones. Genome Biol. 2002;3(2):Reviews1003.
43. Ma J, Svoboda P, Schultz RM, Stein P. Regulation of zygotic gene activation in the preimplantation mouse embryo: global activation and repression of gene expression. Biol Reprod. 2001;64(6):1713–21.
44. Bui HT, Wakayama S, Mizutani E, Park KK, Kim JH, van Thuan N, et al. Essential role of paternal chromatin in the regulation of transcriptional activity during mouse preimplantation development. Reproduction. 2011;141(1):67–77.
45. Sutovsky P, Schatten G. Paternal contributions to the mammalian zygote: fertilization after sperm-egg fusion. Int Rev Cytol. 2000;195:1–65.
46. Tang F, Kaneda M, O'Carroll D, Hajkova P, Barton SC, Sun YA, et al. Maternal microRNAs are essential for mouse zygotic development. Genes Dev. 2007;21(6):644–8.
47. Li L, Zheng P, Dean J. Maternal control of early mouse development. Development. 2010;137(6):859–70.
48. Tsukamoto S, Kuma A, Murakami M, Kishi C, Yamamoto A, Mizushima N. Autophagy is essential for preimplantation development of mouse embryos. Science. 2008;321(5885):117–20.
49. Ferreira EM, Vireque AA, Adona PR, Ferriani RA, Navarro PA. Prematuration of bovine oocytes with butyrolactone I reversibly arrests meiosis without increasing meiotic abnormalities after in vitro maturation. Eur J Obstet Gynecol Reprod Biol. 2009;145(1):76–80.
50. Coticchio G, Dal Canto M, Mignini Renzini M, Guglielmo MC, Brambillasca F, Turchi D, et al. Oocyte maturation: gamete-somatic cells interactions, meiotic resumption, cytoskeletal dynamics and cytoplasmic reorganization. Hum Reprod Update. 2015;21(4):427–54.
51. Jin F, Hamada M, Malureanu L, Jeganathan KB, Zhou W, Morbeck DE, et al. Cdc20 is critical for meiosis I and fertility of female mice. PLoS Genet. 2010;6(9):e1001147.
52. Park DS, Levine B, Ferrari G, Greene LA. Cyclin dependent kinase inhibitors and dominant negative cyclin dependent kinase 4 and 6 promote survival of NGF-deprived sympathetic neurons. J Neurosci. 1997;17(23):8975–83.
53. Copani A, Copani A, Angela Sortino M, Nicoletti F, Bruno V, Nicoletti F, et al. Activation of cell-cycle-associated proteins in neuronal death: a mandatory or dispensable path? Trends Neurosci. 2001;24(1):25–31.
54. Xu X, Lei Y, Luo J, Wang J, Zhang S, Yang XJ, et al. Prevention of beta-amyloid induced toxicity in human iPS cell-derived neurons by inhibition of cyclin-dependent kinases and associated cell cycle events. Stem Cell Res. 2013;10(2):213–27.
55. Duan FH, Chen SL, Chen X, Niu J, Li P, Liu YD, et al. Follicular fluid Abeta40 concentrations may be associated with ongoing pregnancy following in vitro fertilization. J Assist Reprod Genet. 2014;31(12):1611–20.
56. Urieli-Shoval S, Finci-Yeheskel Z, Eldar I, Linke RP, Levin M, Prus D, et al. Serum amyloid a: expression throughout human ovarian folliculogenesis and levels in follicular fluid of women undergoing controlled ovarian stimulation. J Clin Endocrinol Metab. 2013;98(12):4970–8.
57. Boke E, Ruer M, Wühr M, Coughlin M, Lemaitre R, Gygi SP, et al. Amyloid-like self-assembly of a cellular compartment. Cell. 2016;166(3):637–50.
58. Boke E, Mitchison TJ. The balbiani body and the concept of physiological amyloids. Cell Cycle. 2017;16(2):153–4.